catalysts

MDPI

Article

Inorganic Salt Catalysed Hydrothermal Carbonisation (HTC) of Cellulose

James M. Hammerton and Andrew B. Ross *

School of Chemical and Process Engineering, University of Leeds, Leeds LS2 9JT, UK; j.m.hammerton@leeds.ac.uk
* Correspondence: a.b.ross@leeds.ac.uk; Tel.: +44-(0)113-343-1017

Abstract: The presence of inorganic salts either as part of the substrate or added to the reaction medium are known to significantly affect the reaction pathways during hydrothermal carbonisation (HTC) of biomass. This work aims to understand the influence of salts on hydrothermal carbonisation by processing cellulose in the presence of one or more inorganic salts with different valency. Batch experiments and Differential Scanning Calorimetry were used to investigate the change in reaction pathways during hydrothermal conversion. The effect of salts on the rate of HTC of cellulose can be correlated with the Lewis acidity of the cation and the basicity of the anion. The effect of the anion was more pH-dependent than the cation because it can protonate during the HTC process as organic acids are produced. The introduction of salts with Lewis acidity increases the concentration of low molecular weight compounds in the process water. The addition of a second salt can influence the catalytic effect of the first salt resulting in greater levulinic acid yields at the expense of hydrochar formation. Salts also play an important role in cellulose dissolution and can be used to modify the yield and composition of the hydrochars.

Keywords: hydrochar; hydrothermal carbonisation; ash; lignocellulosic biomass; levulinic acid

Citation: Hammerton, J.M.; Ross, A.B. Inorganic Salt Catalysed Hydrothermal Carbonisation (HTC) of Cellulose. *Catalysts* **2022**, *12*, 492. https://doi.org/10.3390/catal12050492

Academic Editor: Francesco Mauriello

Received: 2 March 2022
Accepted: 23 April 2022
Published: 28 April 2022

1. Introduction

As the world moves away from using fossil fuels, there becomes a need for alternative ways of producing energy, chemicals and materials from renewable sources. One option for producing some of these is via hydrothermal conversion routes, which involve the processing of biomass and wastes in hot compressed water. One of the most promising technologies under development is hydrothermal carbonisation (HTC) and involves converting organic material in hot compressed water, below the critical point, into a carbonised solid, commonly known as hydrochar. Water-soluble organic and inorganic compounds, some of which are valuable, are also formed and can be extracted from the process water. Some of the organic material is converted to a gaseous mixture containing mainly carbon dioxide, with smaller amounts of hydrogen, methane, sulphur and nitrogen compounds [1–3].

Cellulose is the most abundant polymer on Earth and consists of glucose monomers joined by glycosidic bonds (β-1 → 4 linkages) in a largely crystalline structure of approximately 3000–15,000 units [4]. The basic chemistry underpinning the hydrothermal carbonisation of cellulose is reasonably well understood and is summarised in Scheme 1 [5]. First, the glycosidic bonds are broken through hydrolysis to produce glucose. This monomer isomerises to fructose and then is dehydrated to 5-hydroxymethylfurfural (HMF). The formed HMF polymerises and undergoes condensation reactions, forming ever higher molecular weight compounds, which eventually precipitate to create hydrochar [6]. Other fragments produced by side reactions are thought to also be incorporated into the structure of hydrochar [6]. This product is sometimes referred to as secondary char or coke [7]. Some studies suggest that hydrochar from cellulose is also produced by solid-solid conversion, where the cellulose directly undergoes dehydration and then polymerisation, forming primary char [8]. It has been reported that secondary char formation is enhanced relative to primary char by high temperatures, solid loading and residence times [9].

There are many organic aqueous products formed through side reactions during hydrothermal carbonisation. Some of the HMF undergoes rehydration to form levulinic acid and formic acid, which are major low molecular weight components of the hydrothermal carbonisation process water [10]. Retro-aldol reactions of glucose occur typically forming C2 and C4 sugars, such as glycolaldehyde and erythrose, and fructose forming C3 sugars (dihydroxyacetone and glyceraldehyde) [11]. From these, other organic compounds form such as lactic, pyruvic and acetic acid [12]. Oxidation of monosaccharides is another potential source of organic acids from the hydrothermal carbonisation process. Zhang et al. [13] reported the oxidation of glucose and cellulose in a 40–60% *w*/*w* $FeCl_3$ solution at 110 °C yielded significant quantities of gluconic, formic and acetic acid, and small quantities of others acids including oxalic, succinic and glyceric acid.

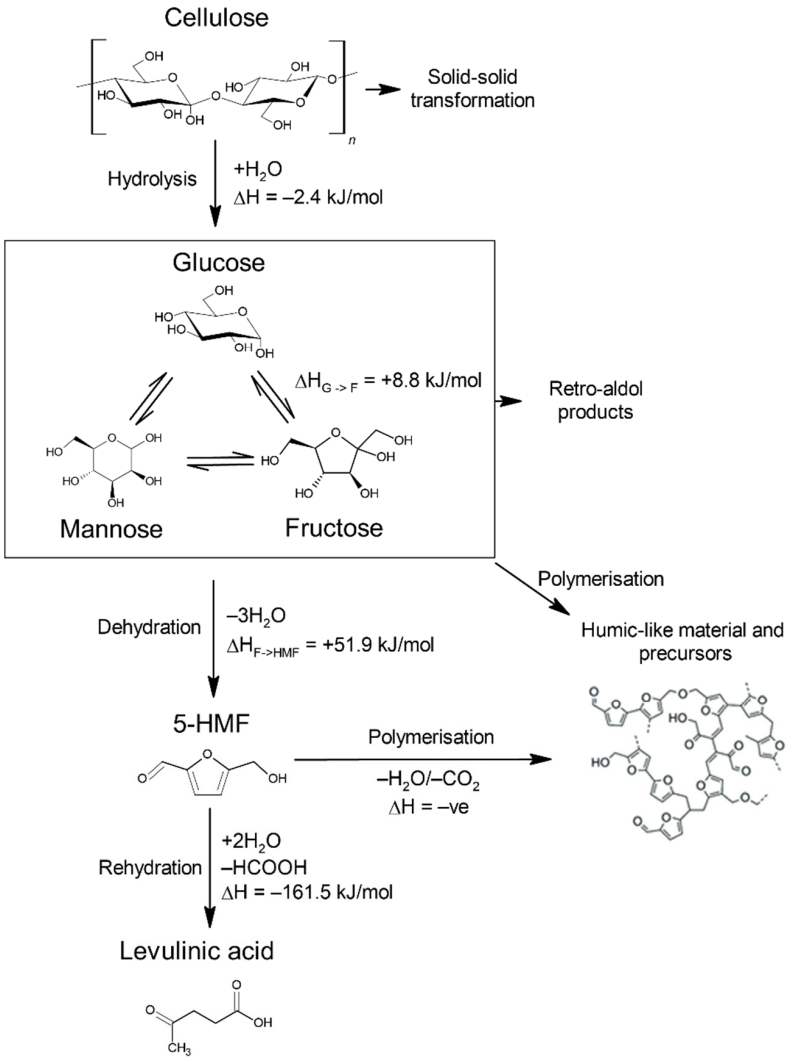

Scheme 1. Main transformations of cellulose during hydrothermal carbonisation and reported enthalpies [14–16].

The hydrochar product (sometimes referred to as biocoal) has been assessed for a range of potential uses. Its utilisation as a solid biofuel is one of the most studied applications because the HTC process converts biomass into a more energy-dense material resembling lignite or sub-bituminous coal [17–19]. Another application being investigated is the utilisation of hydrochar as a soil conditioner [20]. High nutrient feedstocks result in high levels of nitrogen incorporation in the hydrochar making them unsuitable as solid fuels, however, their high levels of nutrients and functionality make them good contenders for soil additives [21–23]. Carbon spheres produced from soluble carbohydrates or intermediate

products have been investigated for use in hydrogen storage, as catalyst supports and as supercapacitors [24,25]. HTC has been investigated on a wide range of feedstocks including wet wastes (such as food waste, sewage sludge and digestate), lignocellulosic biomass and algae [20,26–28].

Inorganic material is often present in HTC for several reasons: It is a constituent of most types of biomass, it may be added to the process to act as a catalyst or the water used may contain dissolved mineral matter, this is particularly the case when process waters are being recycled to minimise water usage. The effect of recycling process waters has been shown to alter the products from HTC. This is caused by the catalytic effect from the organic acids and/or the dissolved mineral matter present [29–31]. Studies using recycled process water have shown increased hydrochar yields, total organic carbon in the process water, carbonisation (in some cases) and energy recovery [29–33].

The addition of acids, alkalis and salts to the reactant water has been shown to alter the distribution of products formed by HTC [34,35]. Rather et al. [35] added KOH, Na_2CO_3 and acetic acid to the HTC reaction and found all influenced the process. The degree of carbonisation increased and mass yield decreased in the following order: No catalyst, acetic acid, Na_2CO_3, KOH. It was not determined what influence these had on the aqueous products. Ming et al. [36] found the presence of sodium salts during the HTC of glucose could enhance the conversion efficiency to carbon spheres and that the anion had a significant effect. Adding different chloride salts to HTC has been shown to influence the reaction pathways taking place. In the presence of chloride salts, the reactor pressure has been reported to decrease which suggests a reduction in decarboxylation reactions is occurring [37,38]. Chloride salts are also known to interfere with hydrogen bonding between cellulose, therefore solubilising more cellulose and improving hydrolysis [39–42].

Most studies in HTC have been performed using thick-walled stainless steel high-pressure batch reactors, often with slow heating and cooling rates, and high thermal inertia making kinetic and enthalpy measurements challenging. Differential scanning calorimetry (DSC) is a tool used to analyse the physical, chemical and thermal properties of materials [43]. It is frequently employed in reaction kinetics and crystallisation studies [44–46]. In recent years, high-pressure crucibles have been developed which allow hydrothermal reactions to be analysed through DSC. Ibbett et al. [47] used a high-pressure DSC technique on lignocellulosic biomass and hydrolysates in the presence of water which found exotherms for the thermal degradation occurred at 223 and 280 °C for hemicellulose and cellulose, respectively. The study found that the temperature of the exotherm related to the decomposition of hemicellulose was approximately 27 °C higher when there was no water present but there was no difference in the case of cellulose.

The enthalpies of several of the important reactions in HTC are summarised in Scheme 1. Hydrolysis of cellulose to glucose is slightly exothermic [16,47,48]. The isomerisation of glucose to fructose, which occurs prior to dehydration, is endothermic [14,15]. The dehydration of fructose to HMF is endothermic and roughly an order greater in magnitude than the previous two steps [14,15,49,50]. Levulinic acid and formic acid formation from the rehydration of HMF is highly exothermic [14,15,51]. Retro-aldol condensation of glucose and fructose, important side reactions, are endothermic and have been calculated to be +50.5 kJ/mol and +46.4 kJ/mol, respectively [52].

The formation of hydrochar from HMF involves several reactions and the structure is not fully understood, however, it is known to be exothermic overall [53,54]. The range of reported heats of reaction from the starting cellulosic biomass to hydrochar is wide because the final product is poorly defined. Funke et al. [55] reported the heat of reaction of hydrothermal carbonisation at 240 °C determined by DSC of glucose and cellulose to be −190.8 kJ/mol and −173.5 kJ/mol, respectively. The similarity of the heat of reaction is interesting considering cellulose can form hydrothermal carbon by two routes, solid-solid transformation and polymerisation of monomers, whereas glucose forms hydrochar only by the latter of the routes. The main difference reported in the study was that the carbonisation of cellulose took longer. Using Hess's law, the maximum heat of reaction from

the hydrothermal carbonisation of cellulose was estimated to be −389.1 kJ/mol [55]. Ischia et al. [56] used DSC and reported heat of reaction of hydrothermal carbonisation of glucose to vary with temperature from −37.8 kJ/mol at 180 °C to −120 kJ/mol at 250 °C which is lower compared to the reported values from Funke et al. [55]. Except for low-temperature hydrothermal carbonisation, the heat of reaction for the conversion of glucose to hydrochar is greater than those reported for the conversion to levulinic acid (−101–−104 kJ/mol) [15].

Predicting the yields of products from the hydrothermal carbonisation of cellulose in complex substrates proves challenging: interactions between intermediaries, macromolecular structure and inorganic constituents add extra levels of complexity. There has been only limited research into the effect of the inorganic constituents of biomass, mainly with the recycling of the aqueous phase, which contains some of the inorganic components, into the HTC process instead of using fresh water [29,32]. This work aims to better understand the effect of the inorganic component in real biomass on the HTC process by adding several different metal salts to a model compound, cellulose. To quantify the effect, High-Pressure Differential Scanning Calorimetry (HP-DSC) is used to monitor the onset of the chemical reactions. Batch experiments combined with post-analysis of the process water and hydrochar are also used to understand the effect of the addition of salts to HTC.

2. Results and Discussion

2.1. Differential Scanning Calorimetry (DSC)

The presence of chloride salts in solution during hydrothermal carbonisation of cellulose was found to significantly affect the temperature at which exothermic reactions began to occur (Figure 1a). All the chloride salts tested were found to decrease this temperature and the effect was more pronounced with cations of greater valency. None of the tests in Figure 1a showed a distinct endotherm prior to the exotherm which means that as HMF was formed, it quickly rehydrated to form levulinic acid or polymerised to hydrochar producing a net exothermic reaction.

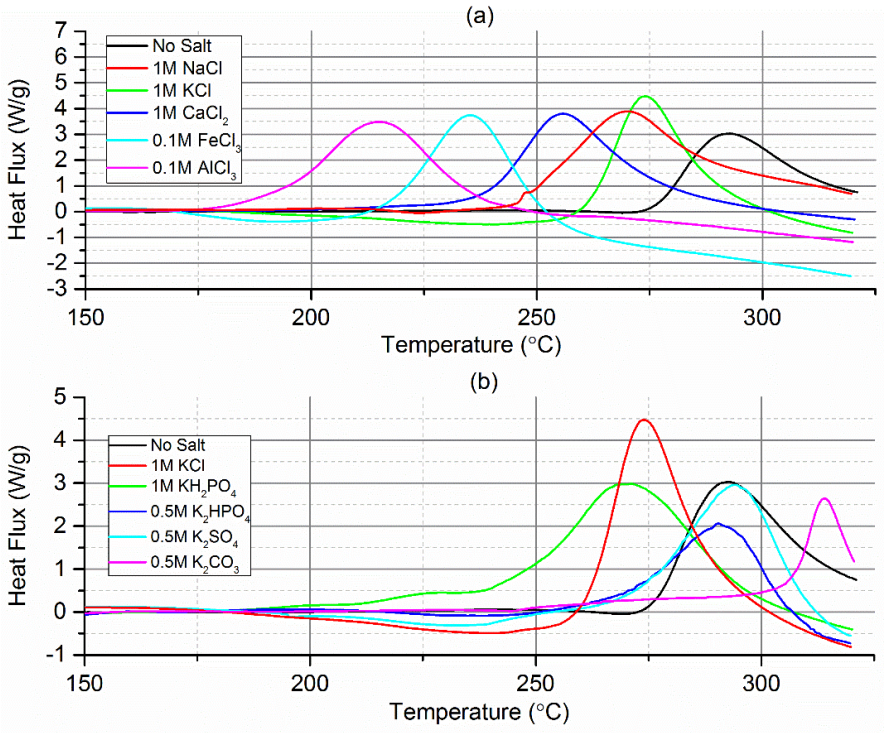

Figure 1. DSC thermograms of the HTC of cellulose in the presence of metal salts. (**a**) Influence of chloride salts, and (**b**) influence of potassium salts.

The anion present also affected the temperature at which exothermic reactions occurred during the hydrothermal carbonisation of cellulose (Figure 1b). K_2CO_3 was the only salt to significantly increase the temperature exothermic reactions occurred in comparison to when no salt was added. This is partially explained by the increase in pH of the reaction medium which is known to suppress hydrothermal carbonisation [57]. K_2CO_3 has been frequently used as a catalyst for hydrothermal liquefaction, which is a process that occurs at higher temperatures, in part because of this observed effect on the lower temperature carbonisation reactions [58–60]. The effect of the potassium salts on the temperature at which the exotherm peaks was ordered by the pH of the respective solutions.

The maxima of the exotherms, shown in Figure 1, were compared to the bonding strength of the cations and anions of the added inorganic salts in Figure 2. The bonding strength is a measure of the Lewis acidity of cations and the basicity of anions [61]. The influence of the chloride salts on the temperature of the maximum heat release strongly correlates with the bonding strength of the cation. Starting pH of the reaction medium was a less important factor-$FeCl_3$ solution (pH 1.69) had a lower pH than $AlCl_3$ (pH 3.67) yet demonstrated a lesser effect on the temperature of maximum heat release. Despite the lower concentration of the iron and aluminium chloride in solution (to preserve the crucibles) compared to the three neutral salts, the influence on the temperature of maximum heat release was greater. $FeCl_3$ had a slightly smaller influence on the temperature of maximum heat release, possibly because the iron reduces during the reaction, as has been reported by Zhang et al. [62]. The effect of H^+ was measured but was not reported in Figure 2 because its small size causes asymmetric two coordination with one strong bond of 0.8 valency units (v.u.) and one weak bond of 0.2 v.u. [63]. For this reason, H^+ is an exceptional cation.

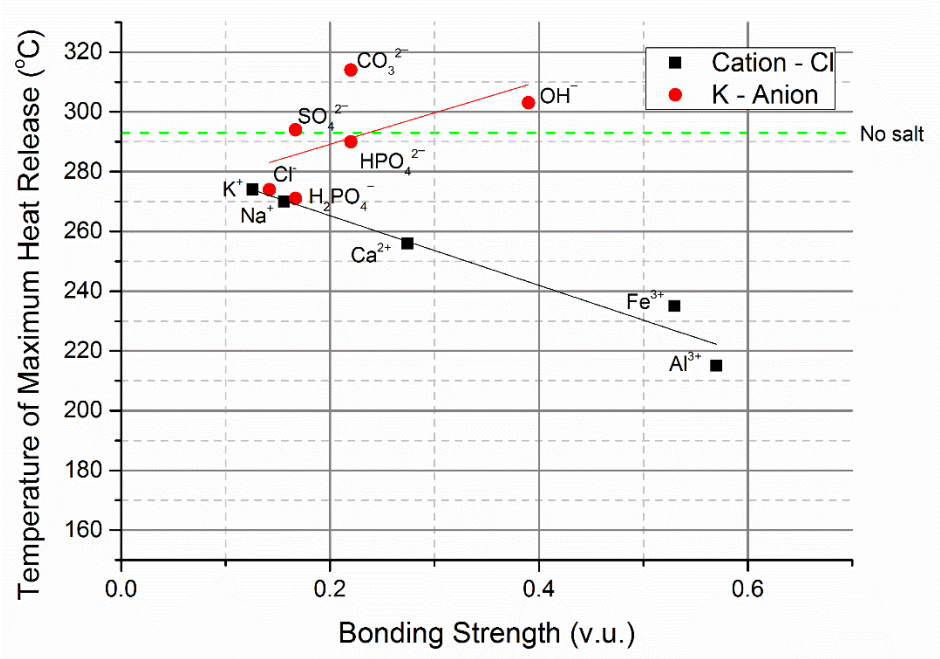

Figure 2. The correlation between ion bonding strength and temperature of maximum heat release determined by DSC. Green dashed line denotes the temperature of maximum heat release when no salt was added. The bonding strength equals valency divided by ideal coordination number [63]. The concentration of K^+ and Cl^- was 1 mol/L, where applicable, except for KOH, $FeCl_3$ and $AlCl_3$ which were added at concentrations of 0.1 mol/L. Fits for both sets of salts produced via linear regression.

The temperature of maximum heat release was found to increase with the bonding strength of the anion, although the correlation was not as strong as with the case of cations. The main reason was that anions reduce bonding strength by protonation, which is expected to occur during hydrothermal carbonisation because organic acids are formed [63,64]. As a

result, the acid dissociation constant (pKa) of the conjugate bases and the pH at the start of the reaction have a marked effect. This was not an issue for the cation dataset because the pKa of the chloride ion is very low, so the concentration does not change as organic acids formed during the process [65]. The bonding strength of hydroxide anions is high, however, these protonate quickly as the concentration of organic acids in the process water increase. In Figure 2, the pairs of anions tested with the same bonding strength (carbonate and hydrogen phosphate, and sulphate and dihydrogen phosphate), the solution with the greatest pH had the highest temperature of maximum heat release. Potassium hydrogen phosphate is slightly basic and significantly protonates when the pH during the reaction reaches the pKa of dihydrogen phosphate (7.21) [66]. This event likely occurs early in the process as the pH must decrease only slightly to reach the pKa, reducing the bonding strength of the anions and explaining why there is little difference in the temperature of maximum heat release when potassium hydrogen phosphate and potassium sulphate were added.

The effect of the pH on the HTC of cellulose was determined by DSC with the addition of HCl or KOH (Figure 3). It was found that the addition of HCl had a more marked effect on the temperature of maximum heat release than KOH. The effect of using a Brønsted acid on the onset of carbonisation was significantly lower than with a strong Lewis acid catalyst.

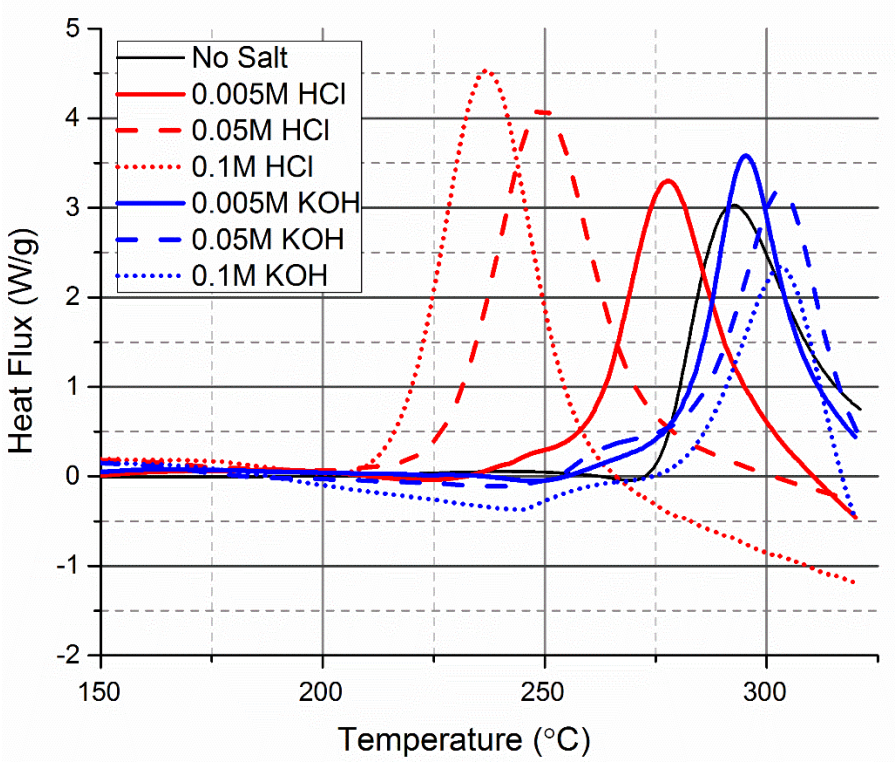

Figure 3. The effect of pH on the HTC of cellulose measured by DSC. pH was decreased or increased with the addition of HCl and KOH, respectively.

The ionic strength of the reaction medium has been identified to influence the hydrothermal carbonisation process [67]. Increasing the concentration of potassium or calcium chloride was found to decrease the temperature at which exothermic reactions occur (Figure 4). When the ionic strength of solutions with the two different salts was balanced (e.g., 3M KCl and 1M $CaCl_2$), the measured heat flux by DSC was different, further showing that Lewis acidity was the major determining factor on the temperature onset of carbonisation. The findings are similar to those reported in Jung et al. [68] which found that quadrupling the concentration of KCl had only a minor effect on the reaction rate constants of HMF conversion to hydrochar and levulinic acid. The presence of $CaCl_2$ instead of KCl

was found to greater increase the reaction rate constants compared to quadrupling the concentration of KCl.

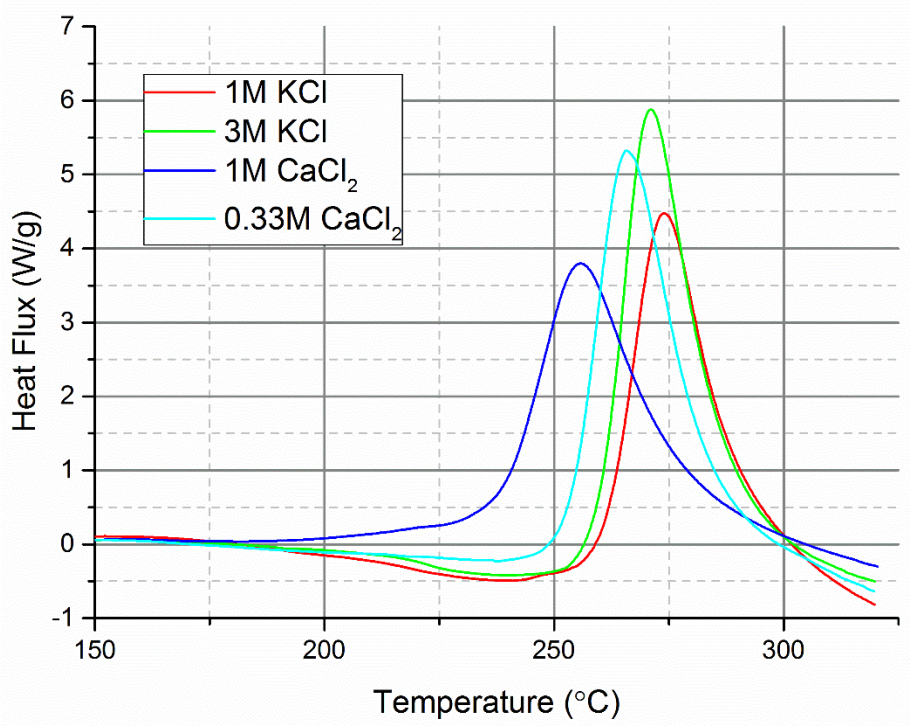

Figure 4. The effect of ionic strength on the HTC of cellulose measured by DSC using two neutral pH chloride salts.

When salts containing the same anion were mixed, the result was the shifting of the exothermic reactions to a temperature between that of when the two salts were used separately in the four mixtures investigated. This presents a potential issue with the hydrothermal carbonisation of real biomass with homogeneous catalysts because inorganic material within the substrate could significantly alter the process. Adding 1M KCl to 0.1M $FeCl_3$ increased the temperature of maximum heat release but further increasing of the concentration of KCl had no further effect on this, although it did increase the overall enthalpy of the reaction (Figure 5a). The observed effect when $CaCl_2$ was added to $FeCl_3$ was similar (Figure 5b). Persson [69] showed that increasing the concentration of chloride ions in an $FeCl_3$ solution changes the distribution of the complexes, reducing the amount of $[Fe(H_2O)_6]^{3+}$ and increasing the concentration of $[FeCl_2(H2O)_4]^+$ when measured at room temperature. Figure 5 provides evidence that the specific complexes formed in solution influence the catalytic ability of the Lewis acid salt which is added. In the presented cases in Figure 5, the distribution of complexes in the aqueous solution was further complicated by the water being superheated, which causes the dielectric constant to decrease and thereby reduces the amount of salt dissociation [70,71]. Elevated temperature also changes the distribution of the complexes [69]. The addition of a second salt also affected the activity of aluminium sulphate, but to a greater extent than was found with the chloride mixtures, with the addition of 0.5M of K_2SO_4 increasing the temperature of maximum heat release to close to the uncatalysed reaction. However, when 0.25M K_2SO_4 was added the effect on the onset of carbonisation appeared to be minimal. The addition of KCl to $AlCl_3$ had a weaker influence on the carbonisation temperature of cellulose than was found with $FeCl_3$, indicating that there were no significant changes to the aluminium species present in solution.

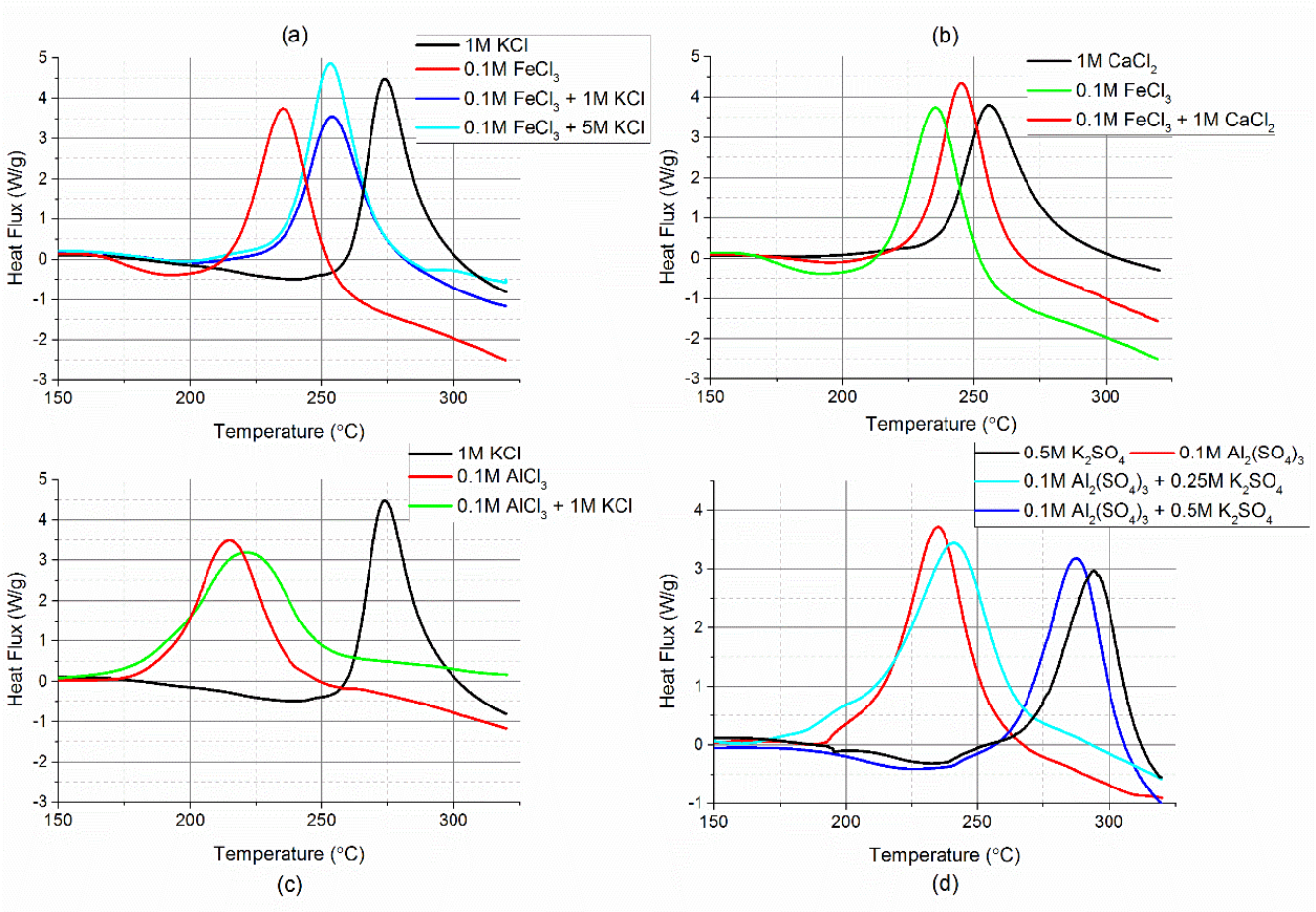

Figure 5. Effect of mixing two salts on the HTC of cellulose. (**a**) iron and potassium chloride, (**b**) iron and calcium chloride, (**c**) aluminium and potassium chloride, and (**d**) aluminium and potassium sulphate.

2.2. Process Water Analysis

Analysis of the process waters, summarised in Table 1, showed that the uncatalysed reaction of cellulose produced few of the key intermediates of the hydrothermal process at the tested reaction conditions. Levulinic acid, an important value-added chemical from biomass, was only detected in the process water when the temperature was raised to 250 °C. The analysis of the process waters when chloride salts were added showed that the key intermediates were formed at gradually lower process temperatures and greater final concentrations as the Lewis acidity increased. Fructose was seldom detected in the process waters because it is quickly dehydrated after production [72]. HMF and furfural were present in process waters formed at moderate temperatures and at low final concentrations, possibly as the long cooling times of the reactor create a period for these to further convert to levulinic acid and hydrochar. Excluding cellulose hydrolysis, glucose conversion to fructose is the limiting step which explains why glucose was the most abundant monosaccharide in the process waters [73]. Epimerisation of glucose to mannose was found to occur when salts were added to the process. Hou et al. [74] also found epimerisation occurred during the hydrothermal conversion of cellulose in the presence of $FeCl_3$.

Table 1. Process water analysis by high-performance liquid chromatography (HPLC). Values reported as mg/L. Dashes denote the analyte was not detected.

Salt	Temperature (°C)	Glucose	Fructose	Mannose	HMF	Levulinic Acid	Furfural	Formic Acid	Acetic Acid
None	100	-	-	-	-	-	-	-	-
	150	-	-	-	-	-	-	-	-
	200	240	120	-	610	-	-	670	-
	250	-	-	-	-	1520	-	460	1100
1M KCl	100	-	-	-	-	-	-	-	-
	150	-	-	-	-	-	-	-	-
	200	10,550	-	500	3480	-	-	630	-
	250	-	-	-	-	8580	-	2220	950
1M $CaCl_2$	100	-	-	-	-	-	-	-	-
	150	2780	-	4060	730	-	-	-	-
	200	-	-	-	-	13,180	-	7180	1210
	250	-	-	-	-	8790	-	1780	1100
0.1M $FeCl_3$	100	6260	-	7590	-	-	-	-	-
	150	5890	-	2320	-	-	-	850	-
	200	-	-	-	-	25,700	-	11,250	770
	250	-	-	-	-	28,380	-	-	1170
0.1M $Al_2(SO_4)_3$	100	-	-	-	-	-	-	-	-
	150	1790	870	-	1450	-	1160	580	-
	200	-	-	-	-	20,080	-	9640	1220
	250	-	-	-	-	18,060	-	-	1310
0.1M $FeCl_3$ + 1M KCl	100	11,900	-	9650	-	-	-	-	-
	150	24,430	-	-	1400	24,580	350	11,660	1770
	200	-	-	-	-	32,690	-	12,690	490
	250	-	-	-	-	31,380	-	-	1330
0.1M $FeCl_3$ + 5M KCl	100	1280	-	4130	-	-	-	-	-
	150	27,920	-	1360	1970	11,250	1960	4820	480
	200	-	-	-	-	31,020	-	13,060	830
	250	-	-	-	-	28,250	-	-	1180
0.1M $FeCl_3$ + 1M $CaCl_2$	100	1790	-	5290	-	-	-	-	-
	150	36,150	560	2230	1440	8870	-	3360	470
	200	-	-	-	-	30,000	-	10,460	500
	250	-	-	-	-	26,880	-	-	1320
0.1M $Al_2(SO_4)_3$ + 0.25M K_2SO_4	100	2940	-	8150	-	-	-	-	-
	150	2960	400	2750	-	-	-	-	-
	200	9060	-	-	2610	8910	-	5190	770
	250	-	-	-	-	3280	-	-	770

The process of rehydration of HMF is known to produce one mole of levulinic acid and one mole of formic acid, but in process waters produced below 250 °C, the detected levels of formic acid were greater than this would suggest. However, most of the formic acid produced was via the rehydration of HMF to levulinic acid. Formic acid: levulinic acid molar ratios greater than one have been reported during the hydrothermal conversion of lignocellulosic materials [64,75]. Formic acid in high quantities has been found, especially in the presence of $FeCl_3$, when oxygen was added to the process [62]. In the present study, air was not removed from the headspace before processing, however, the amount of oxygen available to the reaction was insufficient to fully explain the resulting concentrations. The decomposition of glucose to formic acid and furfuryl alcohol, the latter of which can then polymerise into a hydrochar structure, has been reported as an alternative pathway in aqueous environments in the absence of oxygen [51,75]. The presence of alkali and alkaline metals during pyrolysis has been shown to promote homolytic fission of cellulose to formic acid, smaller oxygenates and furfural, which was also detected in Table 1 [76]. Formic acid may also be produced from the degradation of retro-aldol products of sugars [77]. At process temperatures of 250 °C, formic acid was usually lost and was likely converted to CO_2, which occurs under harsh conditions [78]. The loss of formic acid at high temperatures could be an issue for a biorefinery as many green chemicals require hydrogenation and formic acid is a useful hydrogen carrier.

The mixing of a salt with a trivalent cation and another salt was also found to affect the process water composition. The highest concentrations of monosaccharides, mainly glucose, were found at 150 °C with the addition of KCl and $CaCl_2$ to $FeCl_3$. Levulinic acid production was enhanced by adding a second salt to $FeCl_3$ and the temperature at which

it was produced was reduced to 150 °C. The differences in maximum concentration of levulinic acid achieved in the three $FeCl_3$ samples with an additional salt added were not statistically significant. Jung et al. [79] found that the anion of Brønsted acids participates in the dehydration of fructose and, to a lesser extent, HMF rehydration to levulinic acid, whilst having no significant effect on hydrochar formation. Jung et al. [79] also found that the rate of hydrochar or humin production linearly increased with proton concentration, albeit to a lesser extent than HMF or levulinic acid formation, which suggests that the use of neutral salts could be useful in enhancing reaction rates to improve levulinic acid yields from biomass without also increasing hydrochar formation rates. The process waters with enhanced anion concentration in Table 1 also show fructose dehydration and HMF rehydration reactions becoming more favourable compared to hydrochar formation, causing an increase in levulinic acid concentrations. However, there is a limit at which increasing the anion concentration becomes counter-productive for improving levulinic acid yields shown by greater concentration in the process waters with 1M KCl added to $FeCl_3$ compared to 5M KCl or 1M$CaCl_2$ at lower temperatures. The most promising benefit of increasing anion concentration is the reduction in temperature at which levulinic acid can be formed at significant concentrations, thereby decreasing the heat energy demand of the process. The levulinic acid concentration may be improved further with longer residence times as high concentrations of monosaccharides were present at 150 °C.

The addition of K_2SO_4 to $Al_2(SO_4)_3$ reduced the concentration of levulinic acid in the process water, therefore having the opposite effect to what was observed with the mixed chloride salts. The addition of K_2SO_4 did increase concentrations of monosaccharides which suggests the reduction in levulinic acid concentrations was caused by the reduction in the rate of reaction of dehydration and rehydration steps rather than in the hydrolysis step.

2.3. Hydrochar Analysis

The analysis of hydrochars produced in the presence of inorganic salts is summarised below and in Table S1. The proximate analysis of the hydrochars produced in the presence of a single metal salt followed the behaviour which was predicted by the DSC experiments. The ratio of fixed carbon to volatile matter, which is a measure of the degree of carbonisation in the solid product, began to significantly increase at lower temperatures when metal chloride salts were added to the reaction (Figure 6b). For example, the hydrochars produced at 200 °C had fixed carbon: volatile matter ratios which positively correlated with cation valency. Interestingly, at 250 °C, the ratios were similar for all hydrochars in the presence of chloride salts, as well as when no salt was used, suggesting the observed effect is a rate of reaction increase rather than a change in what carbon structures are formed. The addition of metal chloride salts typically reduced the hydrochar yield (Figure 6a) compared to when no salt was added, which correlates with the increase in aqueous products. Jiang et al. [80] found that the addition of sodium and chloride salts improved cellulose dissolution during hydrothermal processing at 220 °C and that the majority was converted to water-soluble oligomers. The effect was attributed to the salts enhancing depolymerisation and Cl^- ions interrupting the hydrogen bonding network. Salts are well known to affect the solubility of polymers in aqueous solutions and can be used to either "salt-in" or "salt-out" molecules based on whether they interrupt the hydrogen bonding between water molecules (chaotropic) or enhance it (kosmotropic) [81]. Although usually associated with the solubility of proteins, the Hofmeister series of salts is useful for predicting the diameter of hydrochar spheres produced from sucrose in the presence of salts [81]. The mass balance of the solid product in Figure 6a and the concentrations of monomers in Table 1 suggests a large proportion of the cellulose was converted to oligomers or water-soluble medium and high molecular weight material such as humic-like substances [82,83].

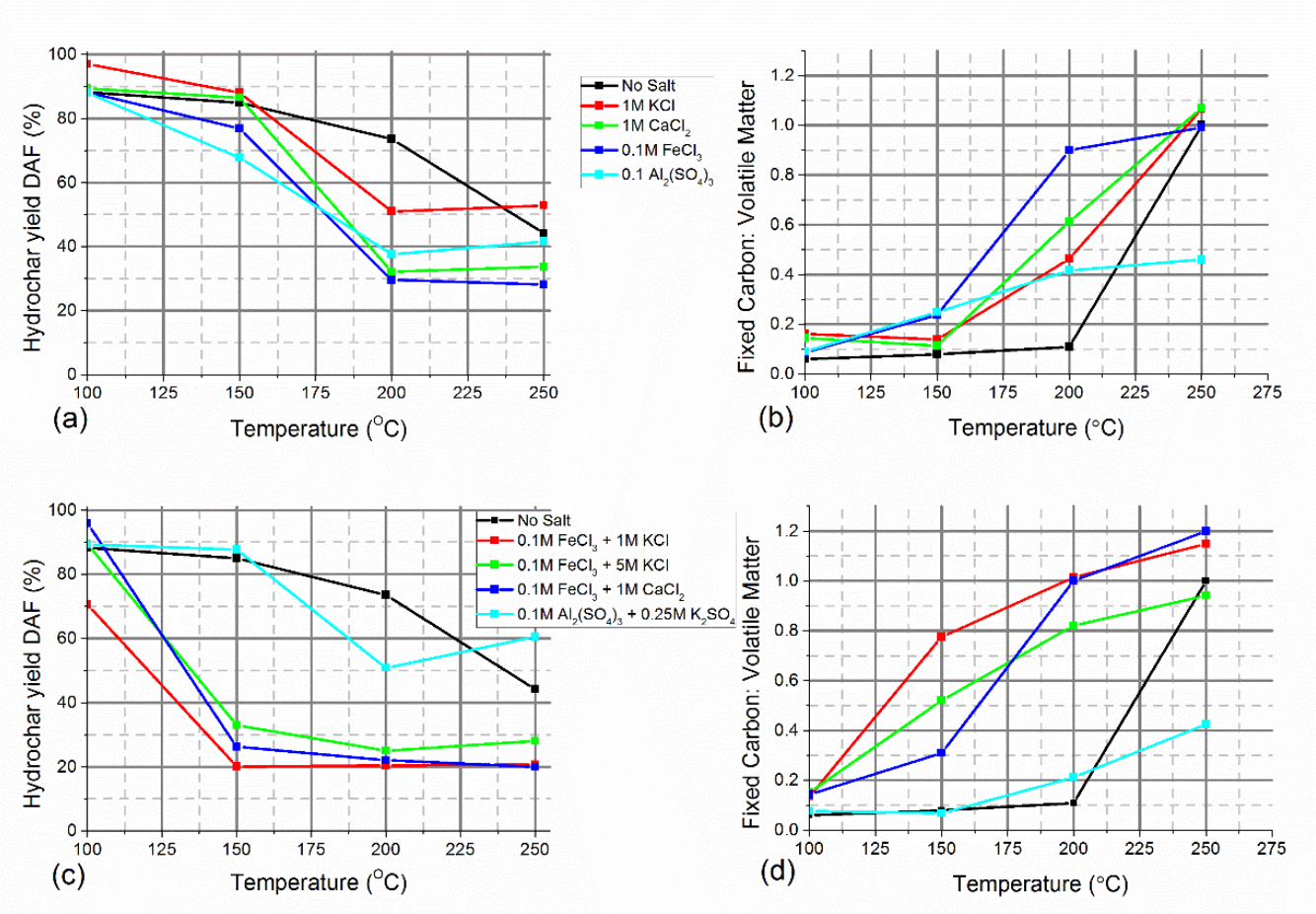

Figure 6. Hydrochar mass yields on a dry ash-free basis (DAF) and the ratio of fixed carbon to volatile matter of the produced hydrochar. (**a**,**b**) hydrochars produced in the presence of a single salt, and (**c**,**d**) produced with a combination of two salts.

The addition of aluminium sulphate to the hydrothermal processing of cellulose was found to have a significant impact on the structure of the hydrochar, which had a lower fixed carbon content than those produced without a salt or in the presence of metal chlorides. This remained the case when K_2SO_4 was also added to the reaction, which reduced the rate of carbonisation and increased the final yield of hydrochar on a dry ash-free basis. The use of metal salts in hydrothermal processing is therefore a promising tool for tuning the properties of hydrochars.

The combination of two chloride salts had a much greater effect on the dissolution of cellulose than when a single salt was used, especially at the lower range of temperatures investigated (Figure 6c). The salts were potentially playing complementary roles, with the high Lewis acidity $FeCl_3$ catalysing key reaction pathways, particularly glucose-fructose isomerisation, and KCl or $CaCl_2$ aiding in solubilising cellulose and thereby improving mass transfer. Both KCl and $CaCl_2$ are generally considered to be chaotropic salts [84,85]. The addition of K_2SO_4, a kosmotropic salt, to $Al_2(SO_4)_3$ increased hydrochar yields across all temperatures.

Whilst DSC experiments showed that the temperature at which carbonisation was occurring increased when a second chloride salt was added to $FeCl_3$ (Figure 6), the fixed carbon: volatile matter ratios of the hydrochars produced at 150 and 200 °C appeared to show the temperature of the onset of carbonisation reduced. This reflected that the uncarbonised cellulose was more likely to be dissolved or depolymerised at these temperatures when a second salt was added, concentrating the insoluble carbonised fraction. The morphology and physical properties of these hydrochars were visually different to those usually formed.

These were noticeably denser and harder than those produced with a single salt, with no salt added, or formed at 250 °C.

In some cases, heightened levels of inorganic material were present in the hydrochars produced despite rinsing with DI water (Table S1). Those produced in the presence of $Al_2(SO_4)_3$ had the highest ash content and contained significant levels of sulphur. $Al_2(SO_4)_3$ is a commonly used flocculant in water treatment, capable of coagulating humic acids which have similarities to hydrochars, and could be playing a similar role in hydrothermal carbonisation [86]. Hydrochars produced in the presence of two chloride salts also contained significant amounts of inorganic material.

The H:C molar ratio of the hydrochars with a single chloride salt further showed carbonisation occurred at lower temperatures with increasing cation valency (Figure 7a). The H:C molar ratio showed the hydrochars with a single chloride salt converged when produced at 250 °C with the hydrochar produced without salt which suggested a similar degree of carbonisation and agrees with the proximate analysis in Figure 6b. Although there were similarities between the hydrochars produced at these temperatures, they may have several differences such as surface area and porosity. The addition of LiCl as a porogen to the hydrothermal carbonisation of lignin has been shown to increase porosity and alter pore size [87]. Using metal chlorides in hydrothermal carbonisation is therefore still a potentially useful strategy for altering the hydrochar structure even at the higher temperature range of the process. When a second chloride salt was added, the molar H:C ratio reduced more at lower processing temperatures when compared to when a single salt was used (Figure 7b). The addition of K_2SO_4 to $Al_2(SO_4)_3$ caused the molar H:C ratio to increase at 150 and 200 °C reflecting the reduction in the dissolution of the depolymerised cellulose fragments. At 250 °C the hydrochars produced in the presence of $Al_2(SO_4)_3$ had low H:C molar ratios, similar to the hydrochars produced under other conditions, showing that dehydration reactions have occurred, despite the final material retaining a low fixed carbon content.

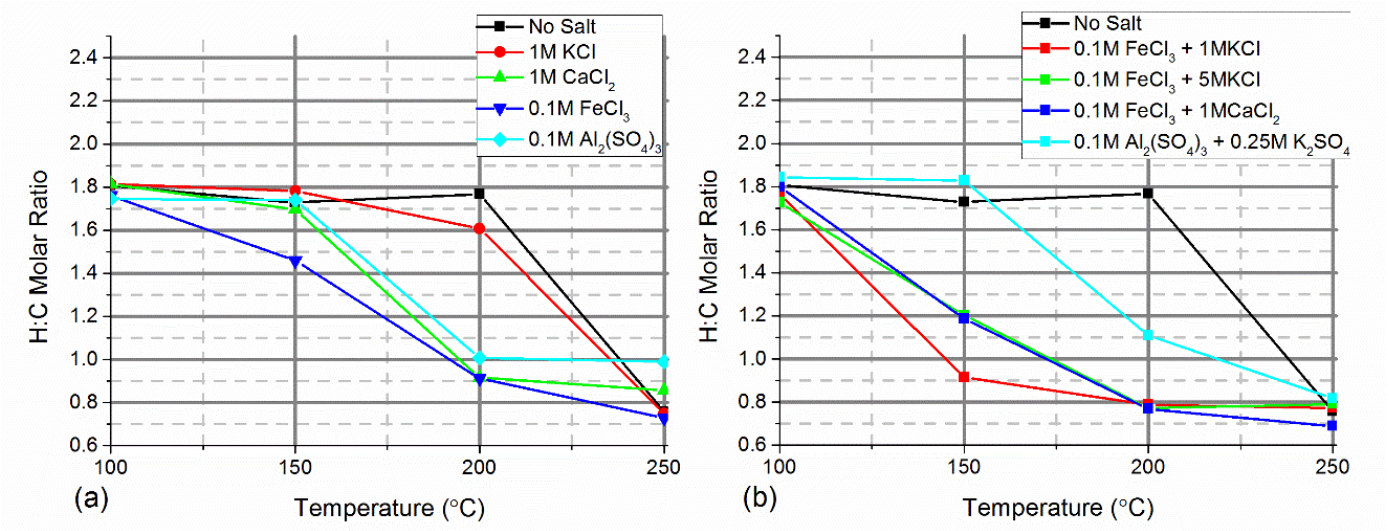

Figure 7. H:C molar ratio of hydrochars with (**a**) a single salt, and (**b**) two salts combined.

3. Materials and Methods

3.1. Materials

Stock solutions were prepared from metal salts of different valency. NaCl, KCl, $CaCl_2$, $FeCl_3$, $AlCl_3$, K_2CO_3, $Al_2(SO_4)_3$, K_2SO_4, K_2HPO_4 and KH_2PO_4 (Sigma-Aldrich, Burlington, MA, USA) were all used. Microcrystalline cellulose (Sigma-Aldrich, Burlington, MA, USA) was used as a model compound. Various concentrations of salts were used from moderate levels, representing concentrations found in recycled process waters, to high levels, which may be added to the process intentionally as a catalyst.

3.2. Methods

3.2.1. HP-DSC

The procedure followed was similar to that in Ibbett et al. [47]. Stainless-steel crucibles with an internal volume of 30 µL and sealed with a gold-plated rupture disc were filled with 3 mg of cellulose and 12 µL of salt-containing solution or deionised water. DSC was performed using a DSC 1 (Mettler Toledo, Columbus, OH, USA). The crucibles were heated from 30 °C to 320 °C at a heating rate of 10 °C/min under a constant flow of 50 mL/min of nitrogen.

3.2.2. HTC Reactions

Larger quantities of hydrochar and process water were made from cellulose and salt solutions using a 600 mL stainless steel reactor and 4843 PID controller (Parr Instrument Company, Moline, IL, USA). 20 g of cellulose was added to 180 g of water plus the appropriate weight of salt before sealing the reactor and heating to the desired reaction temperature at a rate of approximately 8 °C/min. The samples were held at the reaction temperature for 1 h and were cooled slowly at a rate of approximately 2 °C/min. Once cool, the process water was separated with a Buchner funnel and cellulose filter paper, and then stored for further analysis. The solid residue was washed with deionised water to remove any of the remaining salts before being dried in an oven at 60 °C overnight. The mass of the dried residue was recorded. Analysis of a smaller subset found the repeatability of hydrochar yields was within ±3 wt.%.

3.2.3. Proximate and Ultimate Analysis

Moisture, volatile matter, fixed carbon and ash of the produced hydrochars were measured using a TGA/DSC1 (Mettler Toledo, Columbus, OH, USA) according to the method reported in Brown et al. [88]. An alumina crucible was filled with approximately 10 mg of sample. The sample was heated to 105 °C in a nitrogen atmosphere to determine the moisture. Next, the sample was heated to 900 °C for determining the volatile matter. Finally, the atmosphere was changed to air to burn the remaining fixed carbon. The remaining material in the crucible was weighed to determine the ash. Carbon, hydrogen, nitrogen and sulphur in the hydrochars were determined using an EA2000 elemental analyser (Thermo Fisher, Waltham, MA, USA) calibrated against a set of standard materials.The values were adjusted for reporting on a dry basis in accordance with ASTM D3180-1. Proximate and ultimate analysis was performed in duplicate and errors on the measurements are provided in Table S1.

3.2.4. Analysis of Process Waters by HPLC

Before analysis, suspended solids in the process waters were removed with a 0.45 µm syringe filter. The method was used to determine the concentration of monosaccharides, organic acids and furfurals in the process waters. An Ultimate 3000 plus HPLC (Dionex, Sunnyvale, CA, USA) fitted with a Supelcogel C-610H column (Supelco, Bellefonte, PA, USA), refractive index and UV/Vis detector. The injection volume of sample was set to 20 µL. The mobile phase was 0.1% phosphoric acid with a flow rate of 0.5 mL/min. The column oven was maintained at 30 °C throughout the analysis. Concentrations of monosaccharides were quantified using refractive index. Concentrations of organic acids and furfurals were quantified using the UV/Vis detector at a wavelength of 210 nm and 271 nm, respectively. The signal responses were calibrated against a set of standard solutions. Each process water was analysed in triplicate and concentrations of analytes are reported as an average of these. Standard deviations of the analyte concentrations are summarised in Table S2.

4. Conclusions

The addition of salts to the hydrothermal carbonisation of cellulose was found to affect the process in several ways. Firstly, the Lewis acidity of the cation and the basicity of the

anion were found to alter the temperature of the onset of carbonisation independent of pH. The effect of the anion on the process was found to be more complicated than the cation as these protonated as organic acids formed during the process, thereby altering the Lewis basicity. The influence of a Lewis acid on the process was found to be much greater than a Brønsted acid. Secondly, the addition of a salt was found to significantly alter hydrochar yields. This effect was marked when a strong Lewis acid salt was used in conjunction with a neutral salt in high concentration because the neutral salt improved the rate of dehydration and rehydration reactions without affecting the rate of hydrochar formation. Chaotropic salts reduced hydrochar yields, whereas kosmotropic salts slightly increased yields. Finally, the addition of salts increased the concentrations of several compounds in the process water including levulinic acid, a useful platform chemical. Using a combination of salts was found to be a useful approach for increasing the yields of small organic compounds.

Adding a second salt affected the catalytic activity of the first possibly by altering the distribution of complexes that form in solution. This has practical implications for using real biomass in catalysed hydrothermal processes, showing that the solubilisation of ash will alter the reaction kinetics.

Whilst the hydrochars produced at moderate HTC temperatures had varied H:C and fixed carbon: volatile matter ratios, they converged at 250 °C. However, this is not to say that they would not be varied in other ways. The exception was the hydrochar produced with $Al_2(SO_4)_3$ which had significantly less fixed carbon. Overall, adding salts to hydrothermal carbonisation is a useful method for shifting product distributions and tuning the properties of hydrochars.

Supplementary Materials: The following supporting information can be downloaded at: https://www.mdpi.com/article/10.3390/catal12050492/s1, Table S1: Hydrochar yields, proximate and ultimate analysis, Table S2: Process water analysis by HPLC. Average concentration of analytes with standard deviation in brackets.

Author Contributions: Conceptualization, J.M.H. and A.B.R.; Methodology, J.M.H. and A.B.R.; Visualization, J.M.H.; Investigation, J.M.H.; Writing—Original Draft Preparation, J.M.H.; Writing—Review and Editing, J.M.H. and A.B.R.; Supervision, A.B.R. All authors have read and agreed to the published version of the manuscript.

Funding: This research was funded by the UK Catalyst Hub (EPSRC) grant number EP/K014714/1.

Data Availability Statement: All data used is included in the article.

Conflicts of Interest: The authors declare no conflict of interest.

References

1. Mursito, A.T.; Hirajima, T.; Sasaki, K.; Kumagai, S. The effect of hydrothermal dewatering of Pontianak tropical peat on organics in wastewater and gaseous products. *Fuel* **2010**, *89*, 3934–3942. [CrossRef]
2. Funke, A. Fate of Plant Available Nutrients during Hydrothermal Carbonization of Digestate. *Chem. Ing. Tech.* **2015**, *87*, 1713–1719. [CrossRef]
3. Wang, Z.; Zhai, Y.; Wang, T.; Peng, C.; Li, S.; Wang, B.; Liu, X.; Li, C. Effect of temperature on the sulfur fate during hydrothermal carbonization of sewage sludge. *Environ. Pollut.* **2020**, *260*, 114067. [CrossRef] [PubMed]
4. Wang, H.H. Cellulose and Pulp. In *Forests and Forest Plants*; Owens, J.N., Lund, H.G., Eds.; EOLSS Publications: Paris, France, 2009; Volume II, pp. 158–176.
5. Jung, D.; Zimmermann, M.; Kruse, A. Hydrothermal Carbonization of Fructose: Growth Mechanism and Kinetic Model. *ACS Sustain. Chem. Eng.* **2018**, *6*, 13877–13887. [CrossRef]
6. He, Q.; Yu, Y.; Wang, J.; Suo, X.; Liu, Y. Kinetic Study of the Hydrothermal Carbonization Reaction of Glucose and Its Product Structures. *Ind. Eng. Chem. Res.* **2021**, *60*, 4552–4561. [CrossRef]
7. Kruse, A.; Zevaco, T.A. Properties of Hydrochar as Function of Feedstock, Reaction Conditions and Post-Treatment. *Energies* **2018**, *11*, 674. [CrossRef]
8. Lucian, M.; Volpe, M.; Fiori, L. Hydrothermal Carbonization Kinetics of Lignocellulosic Agro-Wastes: Experimental Data and Modeling. *Energies* **2019**, *12*, 516. [CrossRef]
9. Lucian, M.; Volpe, M.; Gao, L.; Piro, G.; Goldfarb, J.L.; Fiori, L. Impact of hydrothermal carbonization conditions on the formation of hydrochars and secondary chars from the organic fraction of municipal solid waste. *Fuel* **2018**, *233*, 257–268. [CrossRef]

10. Qi, Y.; Song, B.; Qi, Y. The roles of formic acid and levulinic acid on the formation and growth of carbonaceous spheres by hydrothermal carbonization. *RSC Adv.* **2016**, *6*, 102428–102435. [CrossRef]
11. Sasaki, M.; Goto, K.; Tajima, K.; Adschiri, T.; Arai, K. Rapid and selective retro-aldol condensation of glucose to glycolaldehyde in supercritical water. *Green Chem.* **2002**, *4*, 285–287. [CrossRef]
12. Nicolae, S.A.; Au, H.; Modugno, P.; Luo, H.; Szego, A.E.; Qiao, M.; Li, L.; Yin, W.; Heeres, H.J.; Berge, N.; et al. Recent advances in hydrothermal carbonisation: From tailored carbon materials and biochemicals to applications and bioenergy. *Green Chem.* **2020**, *22*, 4747–4800. [CrossRef]
13. Zhang, H.; Li, N.; Pan, X.; Wu, S.; Xie, J. Direct Transformation of Cellulose to Gluconic Acid in a Concentrated Iron(III) Chloride Solution under Mild Conditions. *ACS Sustain. Chem. Eng.* **2017**, *5*, 4066–4072. [CrossRef]
14. Antonetti, C.; Licursi, D.; Fulignati, S.; Valentini, G.; Raspolli Galletti, A.M. New Frontiers in the Catalytic Synthesis of Levulinic Acid: From Sugars to Raw and Waste Biomass as Starting Feedstock. *Catalysts* **2016**, *6*, 196. [CrossRef]
15. Assary, R.S.; Redfern, P.C.; Hammond, J.R.; Greeley, J.; Curtiss, L.A. Computational Studies of the Thermochemistry for Conversion of Glucose to Levulinic Acid. *J. Phys. Chem. B* **2010**, *114*, 9002–9009. [CrossRef]
16. Tewari, Y.B.; Goldberg, R.N. Thermodynamics of hydrolysis of disaccharides. Cellobiose, gentiobiose, isomaltose, and maltose. *J. Biol. Chem.* **1989**, *264*, 3966–3971. [CrossRef]
17. Dong, X.; Guo, S.; Wang, H.; Wang, Z.; Gao, X. Physicochemical characteristics and FTIR-derived structural parameters of hydrochar produced by hydrothermal carbonisation of pea pod (*Pisum sativum Linn.*) waste. *Biomass Convers. Biorefinery* **2019**, *9*, 531–540. [CrossRef]
18. Düdder, H.; Wütscher, A.; Stoll, R.; Muhler, M. Synthesis and characterization of lignite-like fuels obtained by hydrothermal carbonization of cellulose. *Fuel* **2016**, *171*, 54–58. [CrossRef]
19. Stirling, R.J.; Snape, C.E.; Meredith, W. The impact of hydrothermal carbonisation on the char reactivity of biomass. *Fuel Processing Technol.* **2018**, *177*, 152–158. [CrossRef]
20. Gupta, D.; Mahajani, S.M.; Garg, A. Investigation on hydrochar and macromolecules recovery opportunities from food waste after hydrothermal carbonization. *Sci. Total Environ.* **2020**, *749*, 142294. [CrossRef]
21. Paneque, M.; De la Rosa, J.M.; Kern, J.; Reza, M.T.; Knicker, H. Hydrothermal carbonization and pyrolysis of sewage sludges: What happen to carbon and nitrogen? *J. Anal. Appl. Pyrolysis* **2017**, *128*, 314–323. [CrossRef]
22. Idowu, I.; Li, L.; Flora, J.R.V.; Pellechia, P.J.; Darko, S.A.; Ro, K.S.; Berge, N.D. Hydrothermal carbonization of food waste for nutrient recovery and reuse. *Waste Manag.* **2017**, *69*, 480–491. [CrossRef] [PubMed]
23. Kruse, A.; Koch, F.; Stelzl, K.; Wüst, D.; Zeller, M. Fate of Nitrogen during Hydrothermal Carbonization. *Energy Fuels* **2016**, *30*, 8037–8042. [CrossRef]
24. Titirici, M.-M.; White, R.J.; Brun, N.; Budarin, V.L.; Su, D.S.; del Monte, F.; Clark, J.H.; MacLachlan, M.J. Sustainable carbon materials. *Chem. Soc. Rev.* **2015**, *44*, 250–290. [CrossRef] [PubMed]
25. Zhao, Y.; Li, W.; Zhao, X.; Wang, D.P.; Liu, S.X. Carbon spheres obtained via citric acid catalysed hydrothermal carbonisation of cellulose. *Mater. Res. Innov.* **2013**, *17*, 546–551. [CrossRef]
26. Aragón-Briceño, C.I.; Ross, A.B.; Camargo-Valero, M.A. Mass and energy integration study of hydrothermal carbonization with anaerobic digestion of sewage sludge. *Renew. Energy* **2021**, *167*, 473–483. [CrossRef]
27. Smith, A.M.; Whittaker, C.; Shield, I.; Ross, A.B. The potential for production of high quality bio-coal from early harvested Miscanthus by hydrothermal carbonisation. *Fuel* **2018**, *220*, 546–557. [CrossRef]
28. Heilmann, S.M.; Davis, H.T.; Jader, L.R.; Lefebvre, P.A.; Sadowsky, M.J.; Schendel, F.J.; von Keitz, M.G.; Valentas, K.J. Hydrothermal carbonization of microalgae. *Biomass Bioenergy* **2010**, *34*, 875–882. [CrossRef]
29. Heidari, M.; Salaudeen, S.; Dutta, A.; Acharya, B. Effects of Process Water Recycling and Particle Sizes on Hydrothermal Carbonization of Biomass. *Energy Fuels* **2018**, *32*, 11576–11586. [CrossRef]
30. Stemann, J.; Putschew, A.; Ziegler, F. Hydrothermal carbonization: Process water characterization and effects of water recirculation. *Bioresour. Technol.* **2013**, *143*, 139–146. [CrossRef]
31. Wang, F.; Wang, J.; Gu, C.; Han, Y.; Zan, S.; Wu, S. Effects of process water recirculation on solid and liquid products from hydrothermal carbonization of Laminaria. *Bioresour. Technol.* **2019**, *292*, 121996. [CrossRef]
32. Uddin, M.H.; Reza, M.T.; Lynam, J.G.; Coronella, C.J. Effects of water recycling in hydrothermal carbonization of loblolly pine. *Environ. Prog. Sustain.* **2014**, *33*, 1309–1315. [CrossRef]
33. Weiner, B.; Poerschmann, J.; Wedwitschka, H.; Koehler, R.; Kopinke, F.-D. Influence of Process Water Reuse on the Hydrothermal Carbonization of Paper. *ACS Sustain. Chem. Eng.* **2014**, *2*, 2165–2171. [CrossRef]
34. Braghiroli, F.L.; Fierro, V.; Parmentier, J.; Vidal, L.; Gadonneix, P.; Celzard, A. Hydrothermal carbons produced from tannin by modification of the reaction medium: Addition of H+ and Ag+. *Ind. Crop. Prod.* **2015**, *77*, 364–374. [CrossRef]
35. Rather, M.A.; Khan, N.S.; Gupta, R. Catalytic hydrothermal carbonization of invasive macrophyte Hornwort (Ceratophyllum demersum) for production of hydrochar: A potential biofuel. *Int. J. Environ. Sci. Technol.* **2017**, *14*, 1243–1252. [CrossRef]
36. Ming, J.; Wu, Y.; Liang, G.; Park, J.-B.; Zhao, F.; Sun, Y.-K. Sodium salt effect on hydrothermal carbonization of biomass: A catalyst for carbon-based nanostructured materials for lithium-ion battery applications. *Green Chem.* **2013**, *15*, 2722–2726. [CrossRef]
37. Lynam, J.G.; Coronella, C.J.; Yan, W.; Reza, M.T.; Vasquez, V.R. Acetic acid and lithium chloride effects on hydrothermal carbonization of lignocellulosic biomass. *Bioresour. Technol.* **2011**, *102*, 6192–6199. [CrossRef] [PubMed]

38. Lynam, J.G.; Toufiq Reza, M.; Vasquez, V.R.; Coronella, C.J. Effect of salt addition on hydrothermal carbonization of lignocellulosic biomass. *Fuel* **2012**, *99*, 271–273. [CrossRef]
39. Gromov, N.V.; Medvedeva, T.B.; Taran, O.P.; Bukhtiyarov, A.V.; Aymonier, C.; Prosvirin, I.P.; Parmon, V.N. Hydrothermal Solubilization–Hydrolysis–Dehydration of Cellulose to Glucose and 5-Hydroxymethylfurfural Over Solid Acid Carbon Catalysts. *Top. Catal.* **2018**, *61*, 1912–1927. [CrossRef]
40. Remsing, R.C.; Swatloski, R.P.; Rogers, R.D.; Moyna, G. Mechanism of cellulose dissolution in the ionic liquid 1-n-butyl-3-methylimidazolium chloride: A 13C and 35/37Cl NMR relaxation study on model systems. *Chem. Commun.* **2006**, *12*, 1271–1273. [CrossRef]
41. Sen, S.; Losey, B.P.; Gordon, E.E.; Argyropoulos, D.S.; Martin, J.D. Ionic Liquid Character of Zinc Chloride Hydrates Define Solvent Characteristics that Afford the Solubility of Cellulose. *J. Phys. Chem. B* **2016**, *120*, 1134–1141. [CrossRef]
42. Yu, Y.; Lou, X.; Wu, H. Some Recent Advances in Hydrolysis of Biomass in Hot-Compressed Water and Its Comparisons with Other Hydrolysis Methods. *Energy Fuels* **2008**, *22*, 46–60. [CrossRef]
43. Ahmadi Khoshooei, M.; Fazlollahi, F.; Maham, Y. A review on the application of differential scanning calorimetry (DSC) to petroleum products. *J. Therm. Anal. Calorim.* **2019**, *138*, 3455–3484. [CrossRef]
44. Furushima, Y.; Nakada, M.; Takahashi, H.; Ishikiriyama, K. Study of melting and crystallization behavior of polyacrylonitrile using ultrafast differential scanning calorimetry. *Polymer* **2014**, *55*, 3075–3081. [CrossRef]
45. Gupta, R.K.; Pant, B.; Agarwala, V.; Sinha, P.P. Differential scanning calorimetry and reaction kinetics studies of $\gamma + \alpha 2$ Ti aluminide. *Mater. Chem. Phys.* **2012**, *137*, 483–492. [CrossRef]
46. Song, M.; Hourston, D.J. An application of modulated-temperature differential scanning calorimetry to the study of crystallisation kinetics in poly(ϵ-caprolactone)-poly(styrene-co-acrylonitrile) blends. *Polymer* **2000**, *41*, 8161–8165. [CrossRef]
47. Ibbett, R.; Gaddipati, S.; Tucker, G. In-situ studies of hydrothermal reactions of lignocellulosic biomass using high-pressure differential scanning calorimetry. *Biomass Bioenergy* **2019**, *121*, 48–55. [CrossRef]
48. Olsen, S.N.; Lumby, E.; McFarland, K.; Borch, K.; Westh, P. Kinetics of Enzymatic High-Solid Hydrolysis of Lignocellulosic Biomass Studied by Calorimetry. *Appl. Biochem. Biotech.* **2011**, *163*, 626–635. [CrossRef]
49. Okano, T.; Qiao, K.; Bao, Q.; Tomida, D.; Hagiwara, H.; Yokoyama, C. Dehydration of fructose to 5-hydroxymethylfurfural (HMF) in an aqueous acetonitrile biphasic system in the presence of acidic ionic liquids. *Appl. Catal. A-Gen.* **2013**, *451*, 1–5. [CrossRef]
50. Zhou, C.; Zhao, J.; Yagoub, A.E.A.; Ma, H.; Yu, X.; Hu, J.; Bao, X.; Liu, S. Conversion of glucose into 5-hydroxymethylfurfural in different solvents and catalysts: Reaction kinetics and mechanism. *Egypt. J. Pet.* **2017**, *26*, 477–487. [CrossRef]
51. Assary, R.S.; Kim, T.; Low, J.J.; Greeley, J.; Curtiss, L.A. Glucose and fructose to platform chemicals: Understanding the thermodynamic landscapes of acid-catalysed reactions using high-level ab initio methods. *Phys. Chem. Chem. Phys.* **2012**, *14*, 16603–16611. [CrossRef]
52. Setzer, W.N. A DFT Analysis of Thermal Decomposition Reactions Important to Natural Products. *Nat. Prod. Commun.* **2010**, *5*, 993–998. [CrossRef] [PubMed]
53. Knežević, D.; van Swaaij, W.P.M.; Kersten, S.R.A. Hydrothermal Conversion of Biomass: I, Glucose Conversion in Hot Compressed Water. *Ind. Eng. Chem. Res.* **2009**, *48*, 4731–4743. [CrossRef]
54. Rebling, T.; von Frieling, P.; Buchholz, J.; Greve, T. Hydrothermal carbonization: Combination of heat of reaction measurements and theoretical estimations. *J. Therm. Anal. Calorim.* **2015**, *119*, 1941–1953. [CrossRef]
55. Funke, A.; Ziegler, F. Heat of reaction measurements for hydrothermal carbonization of biomass. *Bioresour. Technol.* **2011**, *102*, 7595–7598. [CrossRef]
56. Ischia, G.; Cazzanelli, M.; Fiori, L.; Orlandi, M.; Miotello, A. Exothermicity of hydrothermal carbonization: Determination of heat profile and enthalpy of reaction via high-pressure differential scanning calorimetry. *Fuel* **2022**, *310*, 122312. [CrossRef]
57. León, M.; Marcilla, A.F.; García, Á.N. Hydrothermal liquefaction (HTL) of animal by-products: Influence of operating conditions. *Waste Manag.* **2019**, *99*, 49–59. [CrossRef]
58. Belkheiri, T.; Andersson, S.-I.; Mattsson, C.; Olausson, L.; Theliander, H.; Vamling, L. Hydrothermal liquefaction of kraft lignin in sub-critical water: The influence of the sodium and potassium fraction. *Biomass Convers. Biorefinery* **2018**, *8*, 585–595. [CrossRef]
59. Madsen, R.B.; Glasius, M. How Do Hydrothermal Liquefaction Conditions and Feedstock Type Influence Product Distribution and Elemental Composition? *Ind. Eng. Chem. Res.* **2019**, *58*, 17583–17600. [CrossRef]
60. Zhu, Z.; Rosendahl, L.; Toor, S.S.; Chen, G. Optimizing the conditions for hydrothermal liquefaction of barley straw for bio-crude oil production using response surface methodology. *Sci. Total Environ.* **2018**, *630*, 560–569. [CrossRef]
61. Hawthorne, F.C. A bond-topological approach to theoretical mineralogy: Crystal structure, chemical composition and chemical reactions. *Phys. Chem. Miner.* **2012**, *39*, 841–874. [CrossRef]
62. Zhang, H.; Li, N.; Pan, X.; Wu, S.; Xie, J. Oxidative conversion of glucose to gluconic acid by iron(iii) chloride in water under mild conditions. *Green Chem.* **2016**, *18*, 2308–2312. [CrossRef]
63. Brown, I.D. *The Chemical Bond in Inorganic Chemistry: The Bond Valence Model*, 1st ed.; Oxford University Press: New York, NY, USA, 2002; pp. 43–247.
64. Kambo, H.S.; Minaret, J.; Dutta, A. Process Water from the Hydrothermal Carbonization of Biomass: A Waste or a Valuable Product? *Waste Biomass Valorization* **2018**, *9*, 1181–1189. [CrossRef]

65. Makino, T.; Takano, H.; Kamiya, T.; Itou, T.; Sekiya, N.; Inahara, M.; Sakurai, Y. Restoration of cadmium-contaminated paddy soils by washing with ferric chloride: Cd extraction mechanism and bench-scale verification. *Chemosphere* **2008**, *70*, 1035–1043. [CrossRef] [PubMed]
66. Song, H.-L.; Cai, Y.; Wu, Y.; Lu, Y.-X.; Yang, X.-L.; Yang, Y.-L. Enhancing the performance of a bioelectrochemically assisted osmotic membrane bioreactor based on reverse diffusion of organic and buffering draw solutes. *Desalination* **2020**, *496*, 114730. [CrossRef]
67. Lu, X.; Flora, J.R.V.; Berge, N.D. Influence of process water quality on hydrothermal carbonization of cellulose. *Bioresour. Technol.* **2014**, *154*, 229–239. [CrossRef]
68. Jung, D.; Duman, G.; Zimmermann, M.; Kruse, A.; Yanik, J. Hydrothermal carbonization of fructose—effect of salts and reactor stirring on the growth and formation of carbon spheres. *Biomass Convers. Biorefinery* **2021**. [CrossRef]
69. Persson, I. Ferric Chloride Complexes in Aqueous Solution: An EXAFS Study. *J. Solut. Chem.* **2018**, *47*, 797–805. [CrossRef]
70. Akiya, N.; Savage, P.E. Roles of Water for Chemical Reactions in High-Temperature Water. *Chem. Rev.* **2002**, *102*, 2725–2750. [CrossRef]
71. Lee, L.L. *Molecular Thermodynamics of Electrolyte Solutions*, 1st ed.; World Scientific: Singapore, 2008. [CrossRef]
72. Paksung, N.; Pfersich, J.; Arauzo, P.J.; Jung, D.; Kruse, A. Structural Effects of Cellulose on Hydrolysis and Carbonization Behavior during Hydrothermal Treatment. *ACS Omega* **2020**, *5*, 12210–12223. [CrossRef]
73. Garcés, D.; Faba, L.; Díaz, E.; Ordóñez, S. Aqueous-Phase Transformation of Glucose into Hydroxymethylfurfural and Levulinic Acid by Combining Homogeneous and Heterogeneous Catalysis. *ChemSusChem* **2019**, *12*, 924–934. [CrossRef]
74. Hou, Y.; Lin, Z.; Niu, M.; Ren, S.; Wu, W. Conversion of Cellulose into Formic Acid by Iron(III)-Catalyzed Oxidation with O2 in Acidic Aqueous Solutions. *ACS Omega* **2018**, *3*, 14910–14917. [CrossRef] [PubMed]
75. Kammoun, M.; Istasse, T.; Ayeb, H.; Rassaa, N.; Bettaieb, T.; Richel, A. Hydrothermal Dehydration of Monosaccharides Promoted by Seawater: Fundamentals on the Catalytic Role of Inorganic Salts. *Front. Chem.* **2019**, *7*. [CrossRef] [PubMed]
76. Kuzhiyil, N.; Dalluge, D.; Bai, X.; Kim, K.H.; Brown, R.C. Pyrolytic Sugars from Cellulosic Biomass. *ChemSusChem* **2012**, *5*, 2228–2236. [CrossRef] [PubMed]
77. Marianou, A.A.; Michailof, C.C.; Ipsakis, D.; Triantafyllidis, K.; Lappas, A.A. Cellulose conversion into lactic acid over supported HPA catalysts. *Green Chem.* **2019**, *21*, 6161–6178. [CrossRef]
78. Kim, H.S.; Kim, S.-K.; Jeong, G.-T. Efficient conversion of glucosamine to levulinic acid in a sulfamic acid-catalyzed hydrothermal reaction. *RSC Adv.* **2018**, *8*, 3198–3205. [CrossRef]
79. Jung, D.; Körner, P.; Kruse, A. Kinetic study on the impact of acidity and acid concentration on the formation of 5-hydroxymethylfurfural (HMF), humins, and levulinic acid in the hydrothermal conversion of fructose. *Biomass Convers. Biorefinery* **2021**, *11*, 1155–1170. [CrossRef]
80. Jiang, Z.; Yi, J.; Li, J.; He, T.; Hu, C. Promoting Effect of Sodium Chloride on the Solubilization and Depolymerization of Cellulose from Raw Biomass Materials in Water. *ChemSusChem* **2015**, *8*, 1901–1907. [CrossRef]
81. Li, S.; Celzard, A.; Fierro, V.; Pasc, A. Salting Effect in the Hydrothermal Carbonisation of Bioresources. *ChemistrySelect* **2016**, *1*, 4161–4166. [CrossRef]
82. Santos, V.S.; Moura, B.R.; Constantino, I.C.; Metzker, G.; Boscolo, M.; Cornélio, M.L.; Ferreira, O.P.; Mounier, J.L.S.; Hajjoul, H.; Bisinoti, M.C.; et al. Chelating properties of humic-like substances obtained from process water of hydrothermal carbonization. *Environ. Technol. Innov.* **2021**, *23*, 101688. [CrossRef]
83. Yang, F.; Zhang, S.; Cheng, K.; Antonietti, M. A hydrothermal process to turn waste biomass into artificial fulvic and humic acids for soil remediation. *Sci. Total Environ.* **2019**, *686*, 1140–1151. [CrossRef]
84. Metrick, M.A.; MacDonald, G. Hofmeister ion effects on the solvation and thermal stability of model proteins lysozyme and myoglobin. *Colloid Surf. A* **2015**, *469*, 242–251. [CrossRef]
85. Zongo, L.; Lange, H.; Crestini, C. A Study of the Effect of Kosmotropic and Chaotropic Ions on the Release Characteristics of Lignin Microcapsules under Stimuli-Responsive Conditions. *ACS Omega* **2019**, *4*, 6979–6993. [CrossRef] [PubMed]
86. Duan, J.; Wang, J.; Graham, N.; Wilson, F. Coagulation of humic acid by aluminium sulphate in saline water conditions. *Desalination* **2002**, *150*, 1–14. [CrossRef]
87. Li, J.; Li, X.; Han, G.; Liu, C.; Wang, X. Salt-Template Hydrothermal Carbonization for Pd NP-Loaded Porous Carbonaceous Material. *Bioresources* **2019**, *14*, 3630–3650. [CrossRef]
88. Brown, A.E.; Finnerty, G.L.; Camargo-Valero, M.A.; Ross, A.B. Valorisation of macroalgae via the integration of hydrothermal carbonisation and anaerobic digestion. *Bioresour. Technol.* **2020**, *312*, 123539. [CrossRef]